Hall coefficient of Dirac fermions in graphene under charged impurity scatterings

Xin-Zhong Yan[1] and C. S. Ting[2]
[1]*Institute of Physics, Chinese Academy of Sciences, P.O. Box 603, Beijing 100190, China*
[2]*Texas Center for Superconductivity, University of Houston, Houston, Texas 77204, USA*
(Received 22 July 2009; published 9 October 2009)

With a conserving formalism within the self-consistent Born approximation, we study the Hall conductivity of Dirac fermions in graphene under charged impurity scatterings. The calculated inverse Hall coefficient is compared with the experimental data. It is shown that the present calculations for the Hall coefficient and the electric conductivity are in good agreement with the experimental measurements.

DOI: 10.1103/PhysRevB.80.155423 PACS number(s): 73.50.−h, 72.10.Bg, 75.47.−m, 81.05.Uw

I. INTRODUCTION

Since the experiments of graphene were realized,[1–3] much effort has been devoted to studying the transport properties of the Dirac fermions. Many theoretical studies are based on the model of zero-range scatters in graphene.[4–11] However, there is strong evidence that the charged impurities with screened Coulomb potentials[12–14] are responsible for the observed carrier-density dependence of the electric conductivity of graphene.[2] Although the electric conductivity experiment has been successfully explained, so far there existed no microscopic theories to fit the density dependence of inverse Hall coefficient as measured by another experiment in Ref. 2.

In this work, with a conserving formalism within the self-consistent Born approximation (SCBA), the Hall conductivity is calculated by using the diagrams generated from the current-current correlation function. We show that the experimentally measured electric conductivity and the inverse Hall coefficient can both be successfully explained in terms of the carrier scatterings off charged impurities.

At low carrier concentration, the low-energy excitations of electrons in graphene can be viewed as massless Dirac fermions[7,15–17] as being confirmed by recent experiments.[2,3] Using the Pauli matrices σ's and τ's to coordinate the electrons in the two sublattices (a and b) of the honeycomb lattice and two valleys (1 and 2) in the first Brillouin zone, respectively, and suppressing the spin indices for briefness, the Hamiltonian of the system is given by

$$H = \sum_k \psi_k^\dagger v\vec{k}\cdot\vec{\sigma}\tau_z\psi_k + \frac{1}{V}\sum_{kq}\psi_{k-q}^\dagger V_i(q)\psi_k, \tag{1}$$

where $\psi_k^\dagger=(c_{ka1}^\dagger, c_{kb1}^\dagger, c_{kb2}^\dagger, c_{ka2}^\dagger)$ is the fermion operator, the momentum k is measured from the center of each valley, $v(\sim 5.86$ eV Å) is the velocity of electrons, V is the volume of system, and $V_i(q)$ is the charged impurity potential.[14] Here, we neglect the intervalley scatterings in $V_i(q)$ for two reasons. First, for low electron doping, the intervalley scatterings are negligible small than the intravalley ones. Second, by doing so, our formulation of the problem given below will be much simplified. Explicitly, $V_i(q)$ is written as $n_i(-q)v_0(q)\tau_0\sigma_0$ with $n_i(-q)$ and $v_0(q)$ as, respectively, the Fourier components of the impurity density and the electron-impurity potential. For the charged impurity, $v_0(q)$ is given by the Thomas–Fermi (TF) type

$$v_0(q) = \frac{2\pi e^2}{(q+q_{\rm TF})\epsilon}, \tag{2}$$

where $q_{\rm TF}=4k_F e^2/v\epsilon$ is the TF wave number, $k_F=\sqrt{\pi n}$ (with n as the carrier density) is the Fermi wave number, and $\epsilon \sim 3$ is the effective dielectric constant. This model has been successfully used to study the electric conductivity.[14]

Under the SCBA [see Fig. 1(a)],[18,19] the Green's function $G(k,\omega)=[\omega+\mu-v\vec{k}\cdot\vec{\sigma}\tau_z-\Sigma(k,\omega)]^{-1}\equiv g_0(k,\omega)+g_c(k,\omega)\hat{k}\cdot\vec{\sigma}\tau_z$ and the self-energy $\Sigma(k,\omega)$ of the single particles are determined by coupled integral equations[14]

$$\Sigma_0(k,\omega) = \frac{n_i}{V}\sum_{k'} v_0^2(|k-k'|)g_0(k',\omega) \tag{3}$$

$$\Sigma_c(k,\omega) = \frac{n_i}{V}\sum_{k'} v_0^2(|k-k'|)g_c(k',\omega)\hat{k}\cdot\hat{k}' \tag{4}$$

$$g_0(k,\omega) = \tfrac{1}{2}[g_+(k,\omega)+g_-(k,\omega)] \tag{5}$$

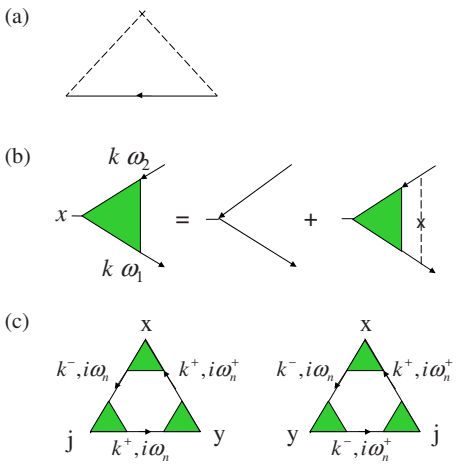

FIG. 1. (Color online) (a) Self-consistent Born approximation for the self-energy. (b) Current vertex with impurity insertions. (c) Diagrams for calculating the Hall conductivity σ_{xy}. The vertex j is associated with the vector potential A_j. $k^\pm=k\pm q/2$. $\omega_n^+=\omega_n+\Omega_m$ with Ω_m and ω_n, respectively, the bosonic and fermionic Matsubara frequencies.

$$g_c(k,\omega) = \tfrac{1}{2}[g_+(k,\omega) - g_-(k,\omega)], \tag{6}$$

where $g_\pm(k,\omega)=[\omega+\mu\mp vk-\Sigma_0(k,\omega)\mp\Sigma_c(k,\omega)]^{-1}$ with μ the chemical potential, $\hat{k}$ is the unit vector in k direction, and the frequency ω is understood as a complex quantity. The chemical potential μ is determined by the doped carrier density n,

$$n = \frac{2}{V}\sum_k \left[-\int_{-\infty}^{\infty} \frac{d\omega}{\pi} F(\omega)\mathrm{Tr\ Im}\, G(k,\omega+i0) - 2 \right] \tag{7}$$

where the front factor 2 comes from the spin degree, the first term in the square brackets is the total occupation of electrons, the last term corresponds to the nondoped case with 2 as the valley degeneracy, and $F(\omega)$ is the Fermi distribution function. We hereafter will call μ determined by Eq. (7) as the renormalized chemical potential, distinguishing from the approximation $\mu \approx E_F = vk_F$ used in some cases such as the semiclassical Boltzmann theory at zero temperature.

Corresponding to the SCBA to the self-energy, the current vertex correction $v\Gamma_x(k,\omega_1,\omega_2)$ is given by the ladder diagrams in Fig. 1(b). $\Gamma_x(k,\omega_1,\omega_2)$ is expanded as

$$\Gamma_x(k,\omega_1,\omega_2) = \sum_{j=0}^{3} y_j(k,\omega_1,\omega_2)A_j^x(\hat{k}), \tag{8}$$

where $A_0^x(\hat{k})=\tau_z\sigma_x$, $A_1^x(\hat{k})=\sigma_x\vec{\sigma}\cdot\hat{k}$, $A_2^x(\hat{k})=\vec{\sigma}\cdot\hat{k}\sigma_x$, $A_3^x(\hat{k})=\tau_z\vec{\sigma}\cdot\hat{k}\sigma_x\vec{\sigma}\cdot\hat{k}$, and $y_j(k,\omega_1,\omega_2)$ are determined by four-coupled integral equations.[14] The functions y_j describe how the current vertex is renormalized by the impurity scatterings from the bare one $A_0^x(\hat{k})$.

II. FORMALISM

We start to calculate the Hall coefficient of the Dirac-fermion system in graphene. Consider that the system is acted with a weak external magnetic field B perpendicular to the graphene plane. The vector potential $\vec{A}(q)$ is related to B via $\vec{B}=i\vec{q}\times\vec{A}(q)$, where $\vec{q}$ is a wave vector. The Hall conductivity σ_{xy} is determined as the ratio between the electric current density along x direction and the electric field E applied in y direction. To find out σ_{xy}, one usually introduces a vector potential $A_y'=cE\exp(-i\Omega t)/i\Omega$ corresponding to E, and calculates the linear response of the current J_x to A_y',

$$\langle \delta J_x(r,t)\rangle = \frac{E}{\hbar\Omega}\int d\vec{r}' \int_{-\infty}^{t} dt' e^{-i\Omega t'}\langle [J_x(r,t),J_y(r',t')]\rangle, \tag{9}$$

where $J_{x,y}(r,t)$ is the current operator, $\langle\cdots\rangle$ means the statistic average. Notice that the average $\langle [J_x(r,t),J_y(r',t')]\rangle$ in the right-hand side of Eq. (9) is under the existence of another vector potential $\vec{A}(q)$ corresponding to the weak magnetic field. Therefore, $\langle \delta J_x(r,t)\rangle$ is expected to have only the component of $\exp([i(\vec{q}\cdot\vec{r}-\Omega t)]$. From Eq. (9), σ_{xy} can be obtained and written as $\sigma_{xy}=-\lim_{\Omega\to 0}\mathrm{Im}\,\Phi_{xy}(\Omega+i0^+)/\Omega$ with $\Phi_{xy}(\Omega)$ as the retarded current-current correlation function. For the Matsubara frequency $\Omega_m=2\pi mT$ with m as a integer, $\Phi_{xy}(i\Omega_m)$ is given by

$$\Phi_{xy}(i\Omega_m) = -\frac{1}{V}\int_0^\beta d\tau e^{i\Omega_m\tau}\langle T_\tau J_x(q,\tau)J_y\ (0,0))\rangle,$$

where T_τ is the τ ordering operator and $J_y(0,0)=J_y(q',\tau')|_{q'=0,\tau'=0}$. Since the Hall coefficient R is defined as $R=\sigma_{xy}/\sigma^2 B$ in the limit $B\to 0$, where σ is the longitudinal electric conductivity at $B=0$, we here consider only the case of very weak magnetic field B and expand the current-current correlation function to the first order of $\vec{A}(q)$. $\Phi_{xy}(i\Omega_m)$ is then obtained as[20,21]

$$\begin{aligned}\Phi_{xy}(i\Omega_m) &= -\frac{1}{V}\sum_j \int_0^\beta d\tau \int_0^\beta d\tau' e^{i\Omega_m\tau}\langle T_\tau J_x(q,\tau)J_y(0,0)\\ &\quad \times J_j(-q,\tau')\rangle A_j(q),\end{aligned} \tag{10}$$

where $\beta=T^{-1}$ with T the temperature and the use of units in which $\hbar=c=k_B=1$ has been made. The statistical average in Eq. (10) is now understood as for the system without any external field. Within SCBA, the function $\Phi_{xy}(i\Omega_m)$ is calculated according to Fig. 1(c). Writing it explicitly, we have

$$\begin{aligned}\Phi_{xy}(i\Omega_m) = \frac{2v^3e^3}{V\beta}\sum_{knj} \mathrm{Tr}\{&[\Gamma_x(k^-,k^+,i\omega_n,i\omega_n^+)G(k^+,i\omega_n^+)\\ &\times\Gamma_y(k^+,k^+,i\omega_n^+,i\omega_n) + \Gamma_y(k^-,k^-,i\omega_n,i\omega_n^-)\\ &\times G(k^-,i\omega_n^-)\Gamma_x(k^-,k^+,i\omega_n^-,i\omega_n)]\\ &\times G(k^+,i\omega_n)\Gamma_j(k^+,k^-,i\omega_n,i\omega_n)G(k^-,i\omega_n)\}A_j(q),\end{aligned} \tag{11}$$

where the factor 2 stems from the spin degeneracy, $k^\pm=k\pm q/2$, and $\omega_n^\pm=\omega_n\pm\Omega_m$. The vertex given by Eq. (8) corresponds to $\Gamma_x(k,k,\omega_1,\omega_2)\equiv\Gamma_x(k,\omega_1,\omega_2)$. $\Gamma_\mu(k^-,k^+,\omega_1,\omega_2)$ satisfies the 4×4 matrix equation

$$\begin{aligned}\Gamma_\mu(k^-,k^+,\omega_1,\omega_2) &= \tau_3\sigma_\mu + \frac{1}{V}\sum_{k_1} n_i v_0^2(k-k_1)G(k_1^-,\omega_1)\\ &\quad\times\Gamma_\mu(k_1^-,k_1^+,\omega_1,\omega_2)G(k_1^+,\omega_2).\end{aligned} \tag{12}$$

$\Gamma_\mu(k^+,k^-,\omega_1,\omega_2)$ is obtained by exchanging $-$ and $+$ in Eq. (12). The analytical continuation $i\Omega_m\to\Omega+i0^+$ for $\Phi_{xy}(i\Omega_m)$ can be manipulated according to the text book.[22] To find out the linearity of σ_{xy} in the magnetic field $\vec{B}=i\vec{q}\times\vec{A}(q)$, we need to expand the right-hand side of Eq. (11) to the first order in q. The expansions of the Green's function $G(k^\pm,\omega)$ and the vertex functions $\Gamma_\mu(k^+,k^+,\omega_1,\omega_2)$ and $\Gamma_\mu(k^-,k^-,\omega_1,\omega_2)$ can be easily obtained. The most involved expansion is for the vertex function $\Gamma_x(k^-,k^+,\omega_1,\omega_2)$. By expanding both sides of Eq. (12), one gets a new integral equation for determining the linear-q term. To the first order in q, $\Gamma_\mu(k^-,k^+,\omega_1,\omega_2)$ is expanded as $\Gamma_\mu(k,\omega_1,\omega_2)+\gamma_\mu(k,q,\omega_1,\omega_2)$ with

$$\gamma_\mu(k,q,\omega_1,\omega_2)=\frac{1}{V}\sum_{k'} n_i v_0^2(k-k')G(k',\omega_1)\gamma_\mu(k',q,\omega_1,\omega_2)\times G(k',\omega_2)-\frac{1}{V}\sum_{k'} n_i v_0^2(k-k')\times[\nabla G(k',\omega_1)\Gamma_\mu(k',\omega_1,\omega_2)G(k',\omega_2) - G(k',\omega_1)\Gamma_\mu(k',\omega_1,\omega_2)\nabla G(k',\omega_2)]\cdot\vec{q}/2, \tag{13}$$

where ∇ means the gradient with respect to k'. For simplifying the final formula for Φ_{xy}, we need to rewrite Eq. (13). From the identity

$$\frac{1}{V}\sum_{kk'} n_i\left[\left(\frac{\partial}{\partial k_j}+\frac{\partial}{\partial k_j'}\right)v_0^2(k-k')\right]\mathrm{Tr}[G(k,\omega_1)\gamma_\mu(k,q,\omega_1,\omega_2)\times G(k,\omega_2)G(k',\omega_2)\Gamma_\nu(k',\omega_2,\omega_1)G(k',\omega_1)]=0, \tag{14}$$

performing the integral by part in the left-hand side of Eq. (14) and using Eq. (13) and the equation for $\Gamma_\nu(k,\omega_1,\omega_2)$, we obtain

$$\sum_k \mathrm{Tr}\left\{\gamma_\mu(k,q,\omega_1,\omega_2)\left[\frac{\partial}{\partial k_j}G(k,\omega_2)\Gamma_\nu(k,\omega_2,\omega_1)G(k,\omega_1) + G(k,\omega_2)\Gamma_\nu(k,\omega_2,\omega_1)\frac{\partial}{\partial k_j}G(k,\omega_1)\right]\right\} = -\frac{\vec{q}}{2}\cdot\sum_k \mathrm{Tr}\left\{[\nabla G(k,\omega_1)\Gamma_\mu(k,\omega_1,\omega_2)G(k,\omega_2) - G(k,\omega_1)\Gamma_\mu(k,\omega_1,\omega_2)\nabla G(k,\omega_2)]\frac{\partial}{\partial k_j}\Gamma_\nu(k,\omega_2,\omega_1)\right\}. \tag{15}$$

On the other hand, the factor $G(k^+,\omega)\Gamma_j(k^+,k^-,\omega,\omega)G(k^-,\omega)$ outside the square brackets in the right hand side of Eq. (11) can be expanded according to

$$vG(k^+,\omega)\Gamma_\alpha(k^+,k^-,\omega,\omega)G(k^-,\omega) = \frac{\partial}{\partial k_\alpha}G(k,\omega)+\frac{\vec{q}}{2}\cdot\sum_j A_j^\alpha(\hat{k})[a_j(k,\omega)\hat{k}+i\sigma_z b_j(k,\omega)\hat{\phi}], \tag{16}$$

where ϕ is the angle of k, $\hat{\phi}$ is the unit vector in ϕ direction, and the use of the Ward identity, $vG(k,\omega)\Gamma_\alpha(k,\omega,\omega)G(k,\omega)=\partial G(k,\omega)/\partial k_\alpha$, has been made. This expansion can be further simplified. If we consider the left-hand side as a functional of the matrices $A_j^\alpha(\hat{k})$, then its transpose should be a functional of matrices $\tilde{A}_j^\alpha(\hat{k})$ defined as $\tilde{A}_0^\alpha(\hat{k})=\tau_z\sigma_\alpha^t$, $\tilde{A}_1^\alpha(\hat{k})=\sigma_\alpha^t\vec{\sigma}^t\cdot\hat{k}$, $\tilde{A}_2^\alpha(\hat{k})=\vec{\sigma}^t\cdot\hat{k}\sigma_\alpha^t$, and $\tilde{A}_3^\alpha(\hat{k})=\tau_z\vec{\sigma}^t\cdot\hat{k}\sigma_\alpha^t\vec{\sigma}^t\cdot\hat{k}$, where σ^t means the transpose of the Pauli matrix. By comparing the transpose of Eq. (16) and the expansion of $vG^t(k^-,\omega)\Gamma_\alpha^t(k^+,k^-,\omega,\omega)G^t(k^+,\omega)$ in terms of $\tilde{A}_j^\alpha(\hat{k})$, we find $a_1=-a_2\equiv a$, $b_1=b_2\equiv b$, and all other a's and b's vanish. Using $\sigma_\alpha\sigma\cdot\hat{k}-\sigma\cdot\hat{k}\sigma_\alpha=-2i\sigma_z\hat{\alpha}\cdot\hat{\phi}$, and $\sigma_\alpha\sigma\cdot\hat{k}+\sigma\cdot\hat{k}\sigma_\alpha=2\hat{\alpha}\cdot\hat{k}$, we obtain

$$vG(k^+,\omega)\Gamma_\alpha(k^+,k^-,\omega,\omega)G(k^-,\omega) = \frac{\partial}{\partial k_\alpha}G(k,\omega)+i\sigma_z\hat{\alpha}\cdot[b(k,\omega)\hat{k}\hat{\phi}-a(k,\omega)\hat{\phi}\hat{k}]\cdot\vec{q}. \tag{17}$$

This result can also be obtained by solving Eq. (13). Since the final result depends on $a(k,\omega)+b(k,\omega)\equiv c(k,\omega)$, we here present only the equations for determining $c(k,\omega)\equiv z(k,\omega)+[g_0^2(k,\omega)-g_c^2(k,\omega)]X(k,\omega)$

$$z(k,\omega)=[g_0'(k,\omega)g_c(k,\omega)-g_0(k,\omega)g_c'(k,\omega)]\times[y_0(k,\omega,\omega)-y_3(k,\omega,\omega)]-g_c(k,\omega)\{g_0(k,\omega)\times[y_0(k,\omega,\omega)+y_3(k,\omega,\omega)]+2g_c(k,\omega)y_1(k,\omega,\omega)\}/k, \tag{18}$$

$$X(k,\omega)=\frac{1}{V}\sum_{k'} n_i v_0^2(k-k')\{z(k',\omega)+[g_0^2(k',\omega)-g_c^2(k',\omega)]X(k',\omega)\}, \tag{19}$$

where $g'(k,\omega)=\partial g(k,\omega)/\partial k$. Using above results, we obtain for the Hall conductivity

$$\sigma_{xy}=\frac{Bv^2e^3}{V}\sum_k\int_{-\infty}^{\infty}\frac{d\omega}{2\pi}\left[-\frac{\partial F(\omega)}{\partial\omega}\right]\times\mathrm{Im}\,\mathrm{Tr}\left\{\Gamma_x^{-+}\left[G^+\left(\frac{\partial\Gamma_y^{+-}}{\partial k_x}\frac{\partial G^-}{\partial k_y}-\frac{\partial\Gamma_y^{+-}}{\partial k_y}\frac{\partial G^-}{\partial k_x}\right)+\left(\frac{\partial G^+}{\partial k_x}\frac{\partial\Gamma_y^{+-}}{\partial k_y}-\frac{\partial G^+}{\partial k_y}\frac{\partial\Gamma_y^{+-}}{\partial k_x}\right)G^- - 2ic(k,\omega^-)G^+\Gamma_y^{+-}\sigma_z\right]\right\}, \tag{20}$$

where $\Gamma_x^{-+}=\Gamma_x(k,\omega^-,\omega^+)$, $\Gamma_y^{+-}=\Gamma_y(k,\omega^+,\omega^-)$, $G^\pm=G(k,\omega^\pm)$, and $\omega^\pm=\omega\pm i0$. In the right-hand side of Eq. (20), terms such as $\Gamma_x^{-+}(\partial G^+/\partial k_x\Gamma_y^{+-}\partial G^-/\partial k_y-\partial G^+/\partial k_y\Gamma_y^{+-}\partial G^-/\partial k_x)$ and those containing the same frequency-ω^+ arguments are not included because they happen to be zero under the operation Im Tr.

III. NUMERICAL RESULT

In a recent work,[23] we have described how to numerically solve Eqs. (3)–(7) and get the solution to the vertex function $\Gamma_\mu(k,\omega_1,\omega_2)$. With these results, the Hall conductivity σ_{xy} can be calculated according to Eq. (20).

The numerical result for the Hall conductivity σ_{xy} normalized by σB as function of carrier concentration δ (doped carrier per carbon atom) is shown in Fig. 2. The solid (red) line is the fully self-consistent calculation with the chemical potential μ determined by the carrier density n, while the dashed (blue) line corresponds to the one of the approximation $\mu\approx E_F\equiv v\sqrt{\pi n}$. For comparison, the Boltzmann result

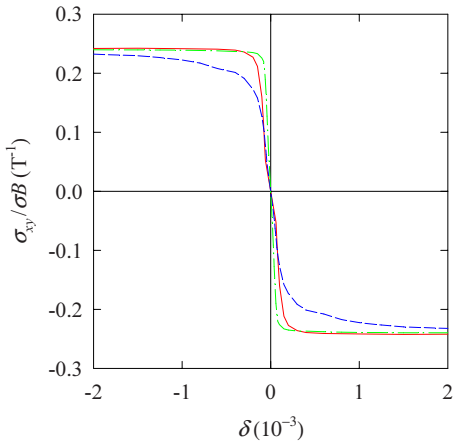

FIG. 2. (Color online) Hall conductivity σ_{xy} normalized by σB as function of the electron-doping concentration δ. σ is the electric conductivity, and B is the magnetic field in unit of Tesla (T). The solid (red) and dashed (blue) lines correspond to the calculation with the renormalized chemical potential μ and the one by $\mu \approx E_F$, respectively. The dot-dashed (green) line is the Boltzmann result.

(normalized with the same σ as for the solid line) is also plotted as the dot-dashed (green) line. Here the impurity density $n_i = 1.15 \times 10^{-3} a^{-2}$ (with a as the lattice constant of graphene) is chosen as the same as in our previous work.[14] This is the only fitting parameter. Within a very narrow range of δ around 0, $\sigma_{xy}/\sigma B$ varies dramatically. Beyond this regime, the saturation behavior of $\sigma_{xy}/\sigma B$ implies that $\sigma_{xy} \propto \sigma \propto \delta$ (for σ see Fig. 3). In the limit $\delta \to 0$, since the normalization denominator is a constant because of the minimum conductivity, σ_{xy} vanishes at $\delta = 0$. Notice that σ_{xy} is an odd function of δ and $\sigma_{xy}/\sigma B$ here is independent of B. The present result differs qualitatively from the low-B limit of Ref. 6. Based on the center migration theory and the delta-type impurity scattering (constant potential in momentum space) model, Ref. 6 studies the Hall conductivity at finite B by incorporating the Landau levels into the Green's function.

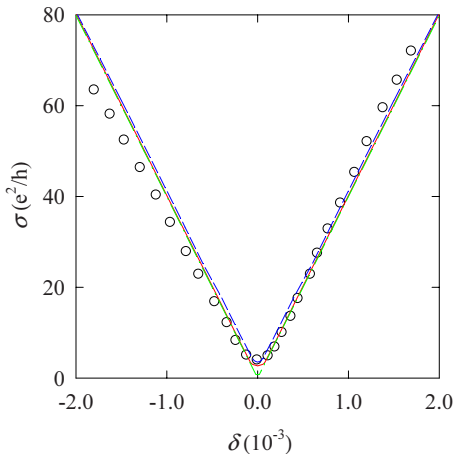

FIG. 3. (Color online) Electric conductivity σ as function of the electron-doping concentration δ. The present calculations are compared with the experimental data in Ref. 2 (symbols). The solid (red), dashed (blue), and dot-dashed (green) lines mean the same as in Fig. 2.

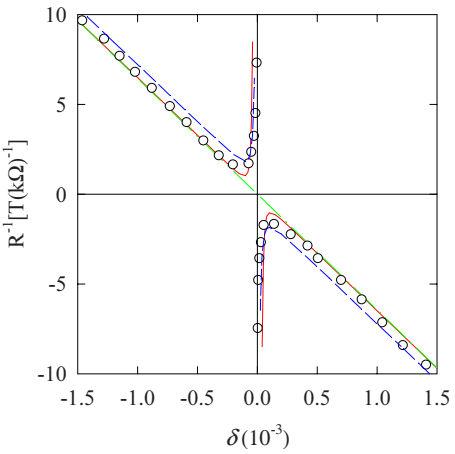

FIG. 4. (Color online) The inverse Hall coefficient R^{-1} (in unit of 10^{-3} T/Ohm) as function of the electron-doping concentration δ. The present calculations are compared with the experimental data in Ref. 2 (symbols). The solid (red), dashed (blue), and the dot-dashed (green) lines mean the same as in Fig. 2.

As $B \to 0$, the spacing of the Landau level becomes vanishing. In this limit, it is found that σ_{xy} as function of the Fermi energy E_F decreases at small positive E_F and after reaching a minimum turns to increasing (with the magnitude deceasing). The difference between the present calculation and Ref. 6 stems predominantly from the electron-impurity scatterings. Also, our result is qualitative different from Ref. 21 in which a constant scattering rate was phenomenologically introduced and the current correlation was treated without vertex correction.

For calculating the Hall coefficient, we need the result of the electric conductivity σ obtained with the same scattering parameters as for σ_{xy}. The results (solid line with the renormalized μ and the dashed line with $\mu \approx E_F$) for σ as functions of δ are shown in Fig. 3 and compared with experimental data.[2] For the minimum conductivity $\sigma_{\min}$, our calculation gives rise to about 2.7 e^2/h using the renormalized μ, and 3.5 e^2/h by $\mu \approx E_F$, both larger than the well-known analytical result 4 $e^2/\pi h$ obtained from the single bubble using the phenomenological scattering rate in the Green's function.[5,10,11] The present calculation also agrees with the numerical computation in Ref. 12 for the conductivity of electron under the charged impurity scatterings, except with $\sigma_{\min}$ larger than that of the latter. It is known that the experimental result of $\sigma_{\min}$ is not universal but depends on the quality of the sample.[24,25] By the present formalism, the minimum conductivity is a consequence of the coherence between the upper and lower band states. For comparison, Fig. 3 also shows the semiclassical Boltzmann result for the electric conductivity (green dot-dashed line), $\sigma_c = E_F \tau e^2/\pi\hbar^2$, with

$$\tau^{-1} = \frac{n_i k_F}{2\pi\hbar v} \int_0^{\pi} d\theta v_0^2 (2k_F \sin\,\theta/2)(1 - \cos^2\,\theta). \quad (21)$$

Clearly, in most region of $\delta > 0$, σ_c is nearly the same as the present result, but goes to zero as $\delta \to 0$.

In Fig. 4, we exhibit the theoretical results for the inverse

Hall coefficient defined as $R^{-1}=B\sigma^2/\sigma_{xy}$ and compare them with the experimental data[2] (symbols). Clearly, the present calculations (solid and dashed lines) fit the experimental measurement of the inverse Hall coefficient as well as the electric conductivity very well. With comparing to the classical prediction $R^{-1}=-nec$, the present theoretical calculations and the experiment data for R^{-1} diverge at $\delta=0$. The divergence of R^{-1} stems from the vanishing of σ_{xy} at $\delta=0$ while the conductivity σ remains finite. The classical theory is based on the concept of the drift velocity. At the zero carrier concentration if the conductivity remains finite, the drift velocity has to become infinitively large, which implies an infinitely large Lorentz force acting on an electron. Actually, $\sigma_{\min}$ vanishes at $\delta=0$ by the classical theory. On the other hand, at large carrier concentration, the present fully self-consistent calculation using the renormalized chemical potential (solid line) reproduces the classical theory, and both of them are in agreement with the experimental result.

Though the classical theory fails to explain the experiment measurement at very low carrier concentration, Hwang *et al.*[26] studied the problem based on the network model of electron-hole puddles using the semiclassical approach. By this model, the local carrier density is finite and the total longitudinal and Hall conductivities are given by the averages of the Boltzmann results in the puddles neglecting the detailed current transferring process between the puddles. The experimentally measured minimum conductivity and the behavior of R^{-1} are so explained.

IV. REMARKS

Before concluding, some remarks are in order. (1) In the present formulation, the single-particle states are treated as the plane waves without taking into account the Landau quantization, since we are considering the $B\rightarrow 0$ limit. (2) The direct electron-electron interaction is neglected here, only partly taken into account in the electron-impurity scattering potential via screening. It is difficult to fully take into account the interelectronic interaction in the electronic transport theory without violating the conservation laws. The conserving approximation is crucial in the microscopic transport theory. Otherwise, any unphysical result could be obtained. On the other hand, since the inner force due to the electron-electron interaction does not change the total momentum, the neglecting of it seems passable when the Coulomb coupling is not strong enough. Actually, the graphene is a weak to moderately coupled Coulomb system.[27] (3) The present calculation is based on the assumption that the impurities are distributed without correlation. However, at very low carrier doping, graphene is an inhomogeneous system due to the interimpurity correlations as observed by experiment.[28,29] There are regions where the carrier concentrations are very low. The resistance comes predominately from these regions. Our calculation at very low carrier concentration can be considered as to study the electron transport in these regions.

V. SUMMARY

In summary, on the basis of self-consistent Born approximation, we have calculated the Hall coefficient of the Dirac fermions under the charged impurity scatterings in graphene. The anomalous in the inverse Hall coefficient at zero carrier concentration stems from the vanishing of the Hall conductivity and meanwhile the minimum remained in the electric conductivity. The latter stems from the quantum coherence effect between the upper and lower Dirac bands. The present results for the inverse Hall coefficient and the electric conductivity are in very good agreement with the experimental measurements.

ACKNOWLEDGMENTS

This work was supported by a grant from the Robert A. Welch Foundation under Grant No. E-1146, the TCSUH, the National Basic Research 973 Program of China under Grant No. 2005CB623602, and NSFC under Grants No. 10774171 and No. 10834011.

[1] K. S. Novoselov, A. K. Geim, S. V. Morozov, D. Jiang, Y. Zhang, S. V. Dubonos, I. V. Grigorieva, and A. A. Firsov, Science **306**, 666 (2004).
[2] K. S. Novoselov, A. K. Geim, S. V. Morozov, D. Jiang, M. I. Katsnelson, I. V. Grigorieva, S. V. Dubonos, and A. A. Firsov, Nature (London) **438**, 197 (2005).
[3] Y. Zhang, Y.-W. Tan, H. L. Stormer, and P. Kim, Nature (London) **438**, 201 (2005).
[4] K. Ziegler, Phys. Rev. Lett. **80**, 3113 (1998).
[5] N. H. Shon and T. Ando, J. Phys. Soc. Jpn. **67**, 2421 (1998); T. Ando, *ibid.* **75**, 074716 (2006).
[6] Y. Zheng and T. Ando, Phys. Rev. B **65**, 245420 (2002).
[7] E. McCann and V. I. Fal'ko, Phys. Rev. Lett. **96**, 086805 (2006).
[8] D. V. Khveshchenko, Phys. Rev. Lett. **97**, 036802 (2006).
[9] I. L. Aleiner and K. B. Efetov, Phys. Rev. Lett. **97**, 236801 (2006).
[10] N. M. R. Peres, F. Guinea, and A. H. Castro Neto, Phys. Rev. B **73**, 125411 (2006).
[11] P. M. Ostrovsky, I. V. Gornyi, and A. D. Mirlin, Phys. Rev. B **74**, 235443 (2006).
[12] K. Nomura and A. H. MacDonald, Phys. Rev. Lett. **98**, 076602 (2007).
[13] E. H. Hwang, S. Adam, and S. Das Sarma, Phys. Rev. Lett. **98**, 186806 (2007).
[14] X.-Z. Yan, Y. Romiah, and C. S. Ting, Phys. Rev. B **77**, 125409 (2008). The conductivity here was not calculated accurately enough near zero carrier concentration. In Fig. 2, y_1 is misdisplayed as $-y_1$.
[15] P. R. Wallace, Phys. Rev. **71**, 622 (1947).
[16] T. Ando, T. Nakanishi, and R. Saito, J. Phys. Soc. Jpn. **67**, 2857 (1998).
[17] A. H. Castro Neto, F. Guinea, and N. M. R. Peres, Phys. Rev. B **73**, 205408 (2006).
[18] E. Fradkin, Phys. Rev. B **33**, 3257 (1986); **33**, 3263 (1986).

[19] P. A. Lee, Phys. Rev. Lett. **71**, 1887 (1993).
[20] H. Fukuyama, H. Ebisawa, and Y. Wada, Prog. Theor. Phys. **42**, 494 (1969).
[21] M. Nakamura and L. Hirasawa, Phys. Rev. B **77**, 045429 (2008).
[22] G. D. Mahan, *Many-Particle Physics*, 2nd ed. (Plenum, New York, 1990), Chap. 7.
[23] X.-Z. Yan, Y. Romiah, and C. S. Ting, arXiv:0904.3303, Phys. Rev. B (to be published).
[24] Y. W. Tan, Y. Zhang, K. Bolotin, Y. Zhao, S. Adam, E. H. Hwang, S. Das Sarma, H. L. Stormer, and P. Kim, Phys. Rev. Lett. **99**, 246803 (2007).
[25] J.-H. Chen, C. Jang, S. Adam, M. S. Fuhrer, E. D. Williams, and M. Ishigami, Nat. Phys. **4**, 377 (2008).
[26] E. H. Hwang, S. Adam, and S. Das Sarma, Phys. Rev. B **76**, 195421 (2007).
[27] X.-Z. Yan and C. S. Ting, Phys. Rev. B **76**, 155401 (2007).
[28] J. Martin, N. Akerman, G. Ulbricht, T. Lohmann, J. H. Smet, K. Von Klitzing, and A. Yacby, Nat. Phys. **4**, 144 (2008).
[29] Y. Zhang, V. W. Brar, C. Girit, A. Zettl, and M. F. Crommie, arXiv:0902.4793 (to be published).